Contamination

AEDC-TR-80-44

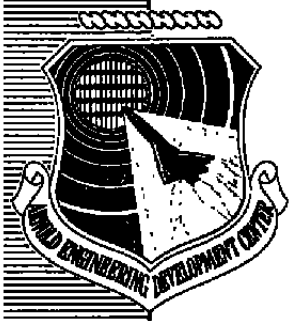

Time- and Space-Dependence of Particulate Effluent in the Exhaust Plume of a Pulsed Liquid Bipropellant Engine

B. P. Curry, J. W. L. Lewis, J. H. Jones
and H. M. Powell
ARO, Inc.

October 1981

Final Report for Period October 1, 1979 – June 30, 1980

Approved for public release; distribution unlimited.

DOC_NUM SER CN
UNC30034-PDC A 1

UNCLASSIFIED

ARNOLD ENGINEERING DEVELOPMENT CENTER
ARNOLD AIR FORCE STATION, TENNESSEE
AIR FORCE SYSTEMS COMMAND
UNITED STATES AIR FORCE

NOTICES

When U. S. Government drawings, specifications, or other data are used for any purpose other than a definitely related Government procurement operation, the Government thereby incurs no responsibility nor any obligation whatsoever, and the fact that the Government may have formulated, furnished, or in any way supplied the said drawings, specifications, or other data, is not to be regarded by implication or otherwise, or in any manner licensing the holder or any other person or corporation, or conveying any rights or permission to manufacture, use, or sell any patented invention that may in any way be related thereto.

Qualified users may obtain copies of this report from the Defense Technical Information Center.

References to named commercial products in this report are not to be considered in any sense as an indorsement of the product by the United States Air Force or the Government.

This report has been reviewed by the Office of Public Affairs (PA) and is releasable to the National Technical Information Service (NTIS). At NTIS, it will be available to the general public, including foreign nations.

APPROVAL STATEMENT

This report has been reviewed and approved.

Norman J. Cochrane

NORMAN J. COCHRANE, Major, USAF
Directorate of Technology
Deputy for Operations

Approved for publication:

FOR THE COMMANDER

Marion L. Laster

MARION L. LASTER
Director of Technology
Deputy for Operations

UNCLASSIFIED

SECURITY CLASSIFICATION OF THIS PAGE (When Data Entered)

REPORT DOCUMENTATION PAGE		READ INSTRUCTIONS BEFORE COMPLETING FORM
1 REPORT NUMBER AEDC-TR-80-44	2 GOVT ACCESSION NO.	3 RECIPIENT'S CATALOG NUMBER
4. TITLE (and Subtitle) THE TIME- AND SPACE-DEPENDENCE OF PARTICULATE EFFLUENT IN THE EXHAUST PLUME OF A PULSED LIQUID BIPROPELLANT ENGINE		5. TYPE OF REPORT & PERIOD COVERED Final Report, October 1, 1979 - June 30, 1980 6 PERFORMING ORG. REPORT NUMBER
7 AUTHOR(s) B. P. Curry, J. W. L. Lewis, J. H. Jones, and H. M. Powell, ARO, Inc., a Sverdrup Corporation Company		8 CONTRACT OR GRANT NUMBER(s)
9 PERFORMING ORGANIZATION NAME AND ADDRESS Arnold Engineering Development Center/DOT Air Force Systems Command Arnold Air Force Station, Tennessee 37389		10 PROGRAM ELEMENT, PROJECT, TASK AREA & WORK UNIT NUMBERS Program Element 65807F
11 CONTROLLING OFFICE NAME AND ADDRESS Arnold Engineering Development Center/DOS Air Force Systems Command Arnold Air Force Station, Tennessee 37389		12 REPORT DATE October 1981 13. NUMBER OF PAGES 22
14 MONITORING AGENCY NAME & ADDRESS(if different from Controlling Office)		15 SECURITY CLASS. (of this report) UNCLASSIFIED 15a DECLASSIFICATION/DOWNGRADING SCHEDULE N/A

16 DISTRIBUTION STATEMENT (of this Report)

Approved for public release; distribution unlimited.

17. DISTRIBUTION STATEMENT (of the abstract entered in Block 20, if different from Report)

18. SUPPLEMENTARY NOTES

Available in Defense Technical Information Center (DTIC).

19 KEY WORDS (Continue on reverse side if necessary and identify by block number)

particulates
dimensions
density
exhaust plumes
high altitude
Mie scattering
jet engines

20 ABSTRACT (Continue on reverse side if necessary and identify by block number)

The temporal and radial profiles of particulate mean sizes and densities in the exhaust plume of a pulsed 5-lbf thrust liquid bipropellant rocket engine have been determined. The primary goal of this analysis has been to establish the capability of simulating the characteristics of multi-second firings at high altitude. The results demonstrate that steady-state particle formulation kinetics are achieved in times on the order of 10 milliseconds. Further,

DD FORM 1 JAN 73 1473 EDITION OF 1 NOV 65 IS OBSOLETE

UNCLASSIFIED

SECURITY CLASSIFICATION OF THIS PAGE (When Data Entered)

20. ABSTRACT, Concluded.

combustion instability was shown to be unimportant for combustion chamber length-to-diameter ratios less than 30. The particle size and flux measurements reported here additionally demonstrate the utility of Mie scattering techniques for pulsed engine testing and contamination tests.

PREFACE

The work reported herein was conducted by the Arnold Engineering Development Center (AEDC), Air Force Systems Command (AFSC). The results were obtained by ARO, Inc., AEDC Group (a Sverdrup Corporation Company), operating contractor for the AEDC, AFSC, Arnold Air Force Station, Tennessee, under ARO Project No. P35K-25. The AEDC project monitor was Dr. Marion Laster. The data analysis was completed on June 15, 1980, and the manuscript was submitted for publication on September 2, 1980.

The authors acknowledge the computational assistance of W. A. Watkins, ARO, Inc.

Authors B.P. Curry, J.W.L. Lewis, and J.H. Jones are currently employed by Calspan Field Services, Inc., AEDC Division. Dr. H.M. Powell is a member of the faculty of Middle Tennessee State University, Murfreesboro, Tennessee.

CONTENTS

ILLUSTRATIONS

Figure

Figure Page

1.0 INTRODUCTION

The verification of the gas dynamic, radiative, and contaminant properties of high altitude rocket exhaust plumes requires the use of ground-based simulation facilities. The accurate, high altitude simulation of these phenomena is, if not impossible, often quite difficult, since the high enthalpy volume flow rate for a multisecond, steady-state firing can exceed greatly the effective pumping speed of the typical cryopumped test chamber. An obvious solution to this problem is the use of short-duration, pulsed engine firings. For this mode of operation the combined advantages of the nonsteady-state behavior of the interaction of the exhaust plume and the proportionately decreased time-integrated volume flow rate into the chamber serve to maintain low chamber pressures during the engine firing and to enable rapid chamber pumpdown between firings. Consequently, simulated high altitude testing capabilities are achieved without the necessity of using a significantly larger cryopumped chamber.

Clearly, to achieve this capability of pulsed engine testing the required diagnostics must possess adequate speed and sensitivity to yield the necessary spatial and temporal resolutions, and, further, the nonsteady behavior of the chamber performance must be understood to define adequately the simulated altitude-versus-time characteristics. Both areas are under active study at the Arnold Engineering Development Center (AEDC). However, an additional obstacle for attaining this capability is ensuring that the pulsed engine exhaust plume of a liquid fuel engine is a faithful representation of the multisecond firing engine exhaust; i.e., steady-state characteristics must be achieved. Order-of-magnitude calculations and experimental data of other work can be provided for typical engines to show that steady state is definitely achieved for development of the nozzle flow, gaseous species combustion, and radiative emission properties. However, central to the feasibility of pulsed engine testing for contamination studies is the question of whether steady-state formation of particulates within the exhaust plume is achieved in short firing times. Specifically, for particulates formed by flow-field condensation processes this question can be addressed analytically. However, the formation of particulates by the incomplete combustion of fuel droplets is much more difficult to predict theoretically, and recourse must be made to experimental studies. The goal of this work was to determine whether steady-state particulate formation existed for short-duration (20- to 100-msec) firings of a 5-lbf-thrust liquid bipropellant engine, the exhaust plume properties of which have been recently studied (Refs. 1 and 2) in the VKF Aerospace Chamber (10V).

2.0 EXPERIMENTAL CONFIGURATION AND THEORY

During this just-mentioned study, as described in Ref. 2, laser scattering was used as a flow visualization technique. The Rayleigh/Mie radiation scattered by the flow field from incident pulsed ruby laser beam was detected by an image intensifier-vidicon system. The laser beam was injected into the flow field perpendicular to the flow axis at a distance of 1.1 in. (2.8 cm) from the nozzle exit and, using the intensifier, observations in the radial direction of ± 0.735 in. (± 1.88 cm) relative to the centerline were performed with a spatial resolution of 0.1 in. (0.25 cm). The image intensifier viewed the plume at 90 deg with respect to both the illuminating laser beam and the plume axis, and the incident laser polarization axis was oriented very nearly antiparallel to the scattering plane (plane of the incident and scattered light propagation vectors).

Data were acquired with a nominal time resolution of 1 msec. For the majority of the data acquired the laser scattering signal was unpolarized. However, during the investigation of an engine exhaust combustion pulse of a nominal 20-msec duration, the degree of polarization of the scattered radiation was determined at the times t = 17 msec and 60 msec, the latter point occurring in the post-shutdown phase of the burn. (The times quoted in this work, as in Ref. 2, are relative to the leading edge of the electrical pulse which opens the propellant valves.)

Using the experimental apparatus described in Ref. 2 and a calibration procedure which used the Rayleigh scattering from N_2 at a known temperature and pressure, the unpolarized Rayleigh/Mie scattered radiation was used to provide spatially and temporally resolved values of the product of number density, n, and scattering cross section, $\sigma(\bar{x})$, corresponding to the particle size distribution function (PSDF) of the effluent. The average size parameter, $(\bar{x})$, is defined in terms of the mean diameter, $\bar{D}$, and laser wavelength, λ, to be

$$\bar{x} = \pi \bar{D} / \lambda$$

Since the purpose of the laser scattering measurements of the exhaust plume was flow visualization rather than particulate characterization, insufficient data exist to determine independent values of n and σ, which depend on the particulate mean size parameter and index of refraction, η. Consequently, $n\sigma$ must serve as a measure of the time dependence of the particulate properties; i.e., if $n\sigma$ is found to be constant in time it will be assumed that both n and σ (and, therefore, $\bar{D}$) are all constant. It is recognized that it is possible, in principle, that a constant $n\sigma$ product can be obtained for time-varying values of n and σ, but such a coincidence is assumed not to be the case. Moreover,for particle size distribution functions of comparatively narrow width, it can be shown that for $\bar{x}$ values on the order of 2 and less, with approximately a factor of two (2) uncertainty,

$$\sigma \approx \overline{D^3}$$

In the absence of information on the shape of the PSDF, we assume that $\overline{D^3} = (\overline{D})^3$ and that $\overline{D}$ will be obtained from the analysis of the polarized scattered light. Thus,

$$n\sigma \approx \rho_p$$

where ρ_p is the particulate mass density within the flow field. Therefore, one can regard the measured values of $n\sigma$ as a measure of the mass density of particulates. It is seen that a time-independent behavior of $n\sigma$ implies a constant value of ρ_p, from which time-independent values of n and $\overline{D}$ are assumed.

The polarization-specific data acquired at 17 msec in one set of measurements were used to determine (Refs. 2 and 3) the average size parameter, $\bar{x}$. Assuming $\bar{x}$ to be constant throughout the engine combustion period, local values of n were determined, which, when combined with estimates of the flow speed, v_∞, yielded estimates of the particulate flux density, J_p, where

$$J_p = n v_\infty$$

3.0 RESULTS AND DISCUSSION

3.1 LASER SCATTERING RESULTS

Shown in Figs. 1 through 7 are the variations with engine firing time of the $n\sigma$ product for the radial, or vertical, region 0.735 in. (-1.88 cm) $\leq y \leq$ 0 in., and it is seen that for all off-axis locations the product of number density and average cross section reaches a steady-state value in less than 30 msec. Further, for radial positions $|y| \lesssim 0.625$ in. (1.57 cm), steady state is attained in less than 20 msec. Similar results were found for all other cases studied. Insofar as this project is concerned, the project goal has been satisfied at this point in that the particulate properties as manifested by the $n\sigma$ product have been shown to reach a steady-state condition in times on the order of 20 to 30 msec. However, it is of interest with regard to the implications of these data for both short-pulse engine testing and contamination tests to analyze further the data in-hand. Figure 8 shows the radial profile of the $n\sigma$ product at 42.5 msec of the engine burn, and it is seen that the particulate effluent is slightly asymmetric.

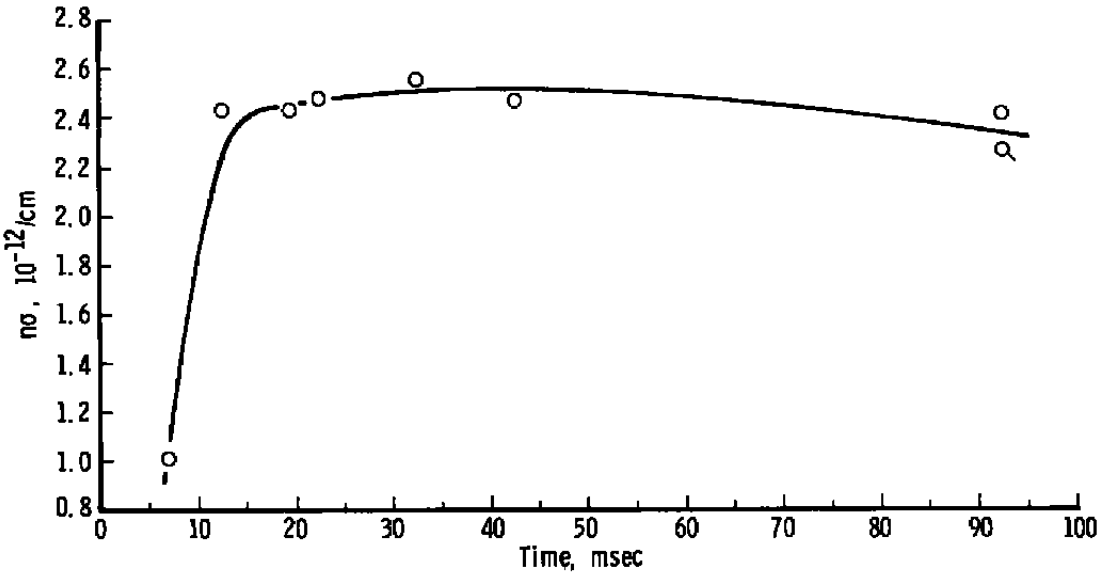

Figure 1. Centerline temporal variation of particulate nσ product.

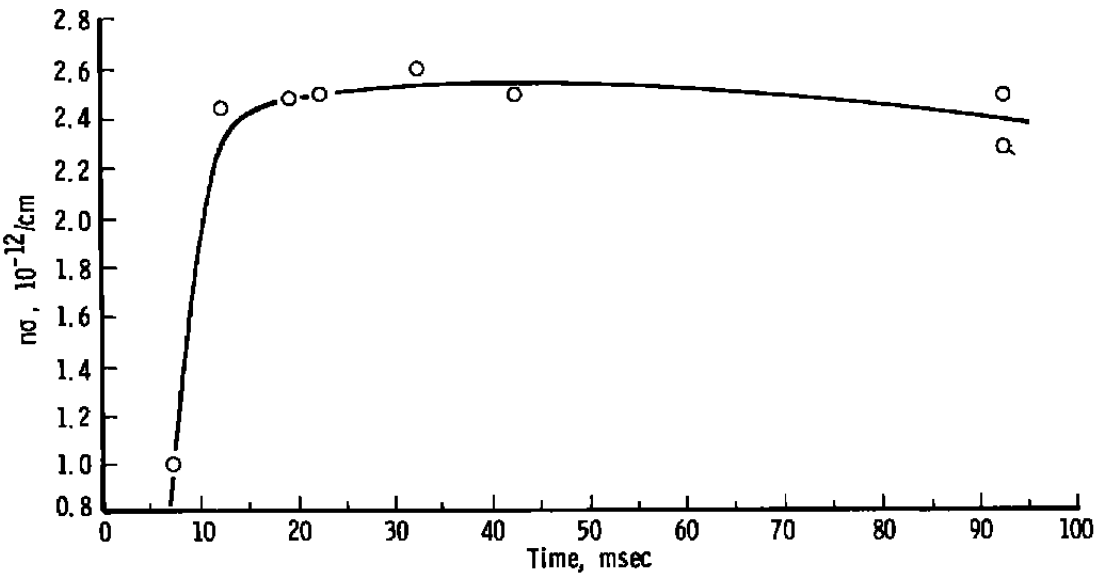

Figure 2. Off-axis temporal variation of particulate nσ product (0.1225 in. below centerline).

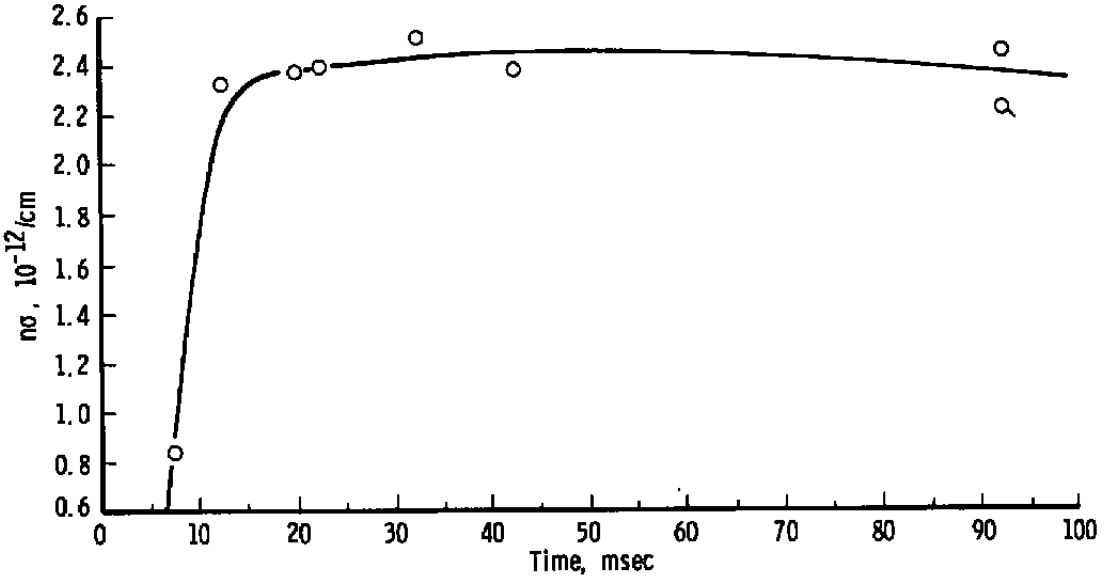

Figure 3. Off-axis temporal variation of particulate nσ product (0.245 in. below centerline).

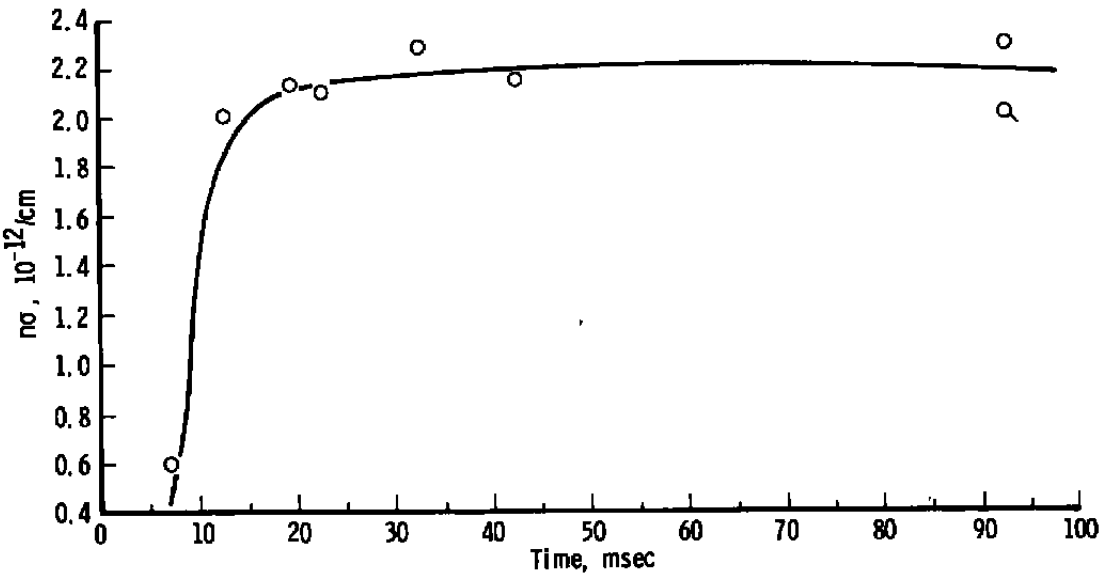

Figure 4. Off-axis temporal variation of particulate nσ product (0.3675 in. below centerline).

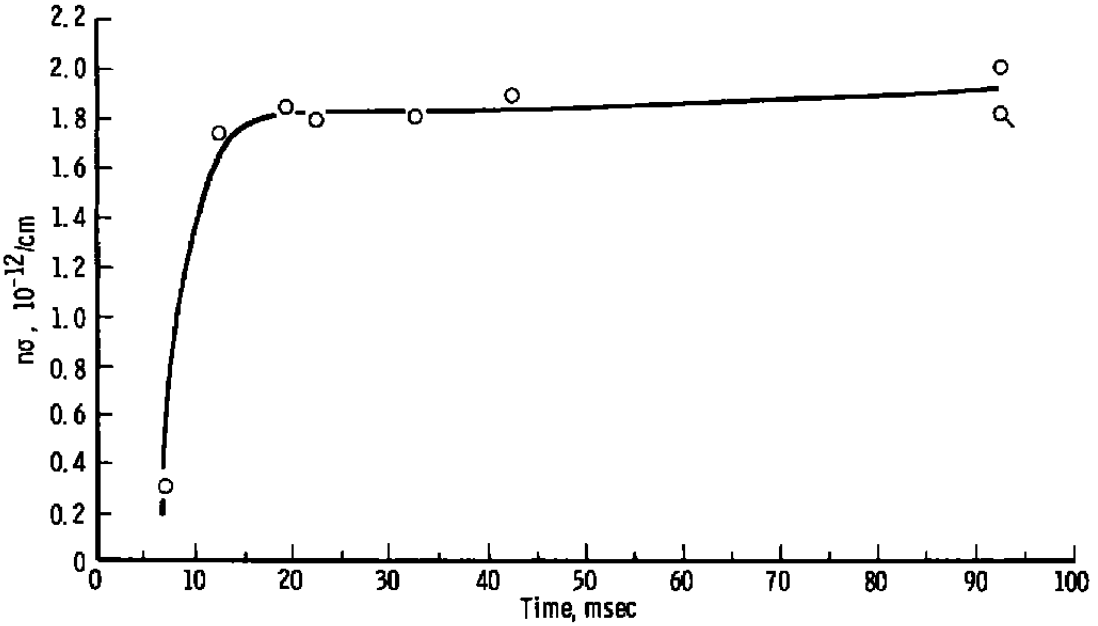

Figure 5. Off-axis temporal variation of particulate nσ product (0.49 in. below centerline).

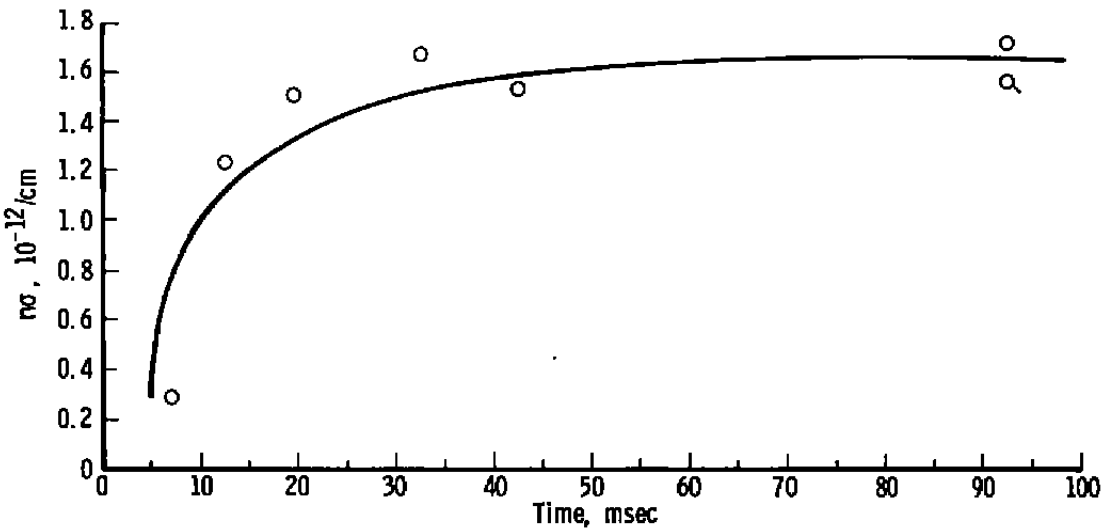

Figure 6. Off-axis temporal variation of particulate nσ product (0.625 in. below centerline).

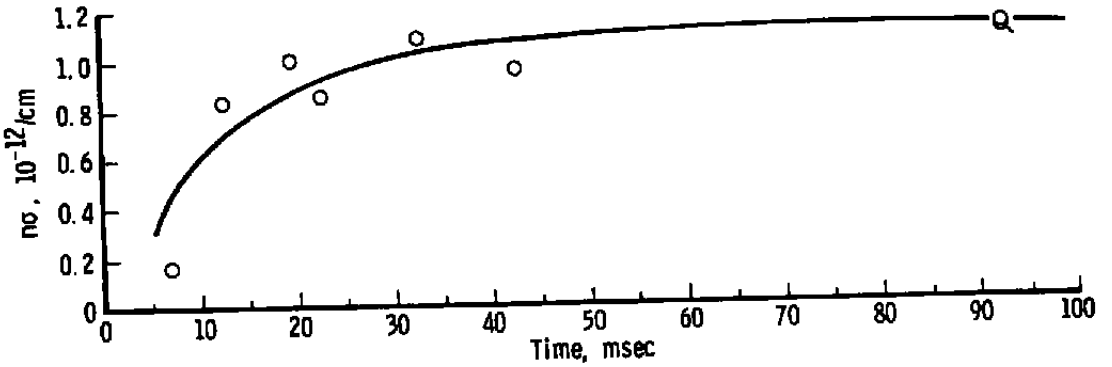

Figure 7. Off-axis temporal variation of particulate nσ product (0.735 in. below centerline).

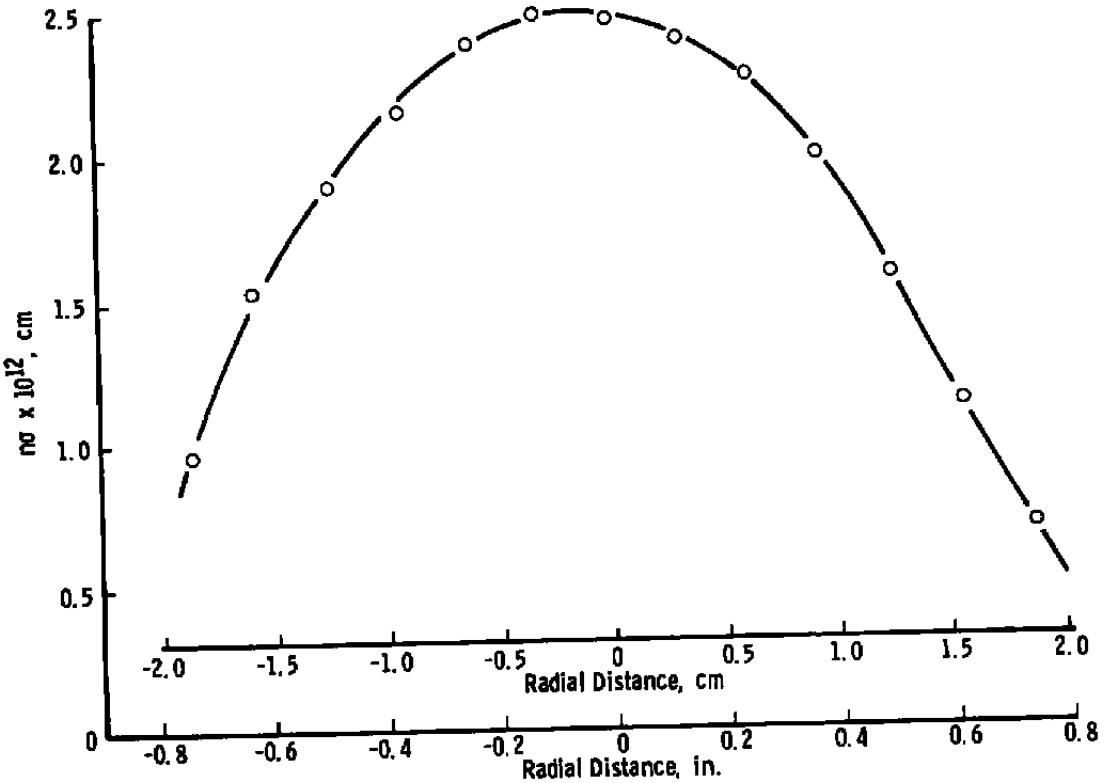

Figure 8. Radial variation of particulate nσ product.

The average particle size parameter ($\bar{x}$) was determined using the degree of polarization (P) measurements obtained at the scattering angle of 90 deg. The angle (ϕ) between the scattering plane and the polarization vector of the incident laser was 177 deg (rather than the design value of 180 deg). As discussed in Refs. 2 and 3, the size parameter results are dependent upon the index of refraction (η) of the particle. Since the particulate material was assumed to be unburned liquid fuel droplets, the index of refraction used was appropriate for that of liquid species. Figure 9 shows the variation of P with $\bar{x}$ for an index of refraction of 1.2 for ϕ = 177 deg. Also shown in Fig. 9 is the experimentally determined value of P for a typical centerline measurement. It is seen that, for this case, $\bar{x} = 2.08^{+0.04}_{-0.06}$, which corresponds to $\overline{D} = 0.45 \pm 0.01\mu m$. Figures 10 and 11 show similar results for η = 1.335 and 1.5, respectively, and Fig. 12 shows the inaccuracy in $\bar{x}$ (and $\overline{D}$) caused by the uncertainty in η. It is seen from Fig. 12 that, using η = 1.335, which is a value characteristic for low viscosity liquids, $\bar{x} \pm \Delta\bar{x} = 1.70^{+0.16}_{-0.22}$. Consequently, the inaccuracy in $\bar{x}$ due to the uncertainty in η is on the order of ±30 percent, which significantly exceeds the uncertainty in $\bar{x}$ caused by experimental imprecision.

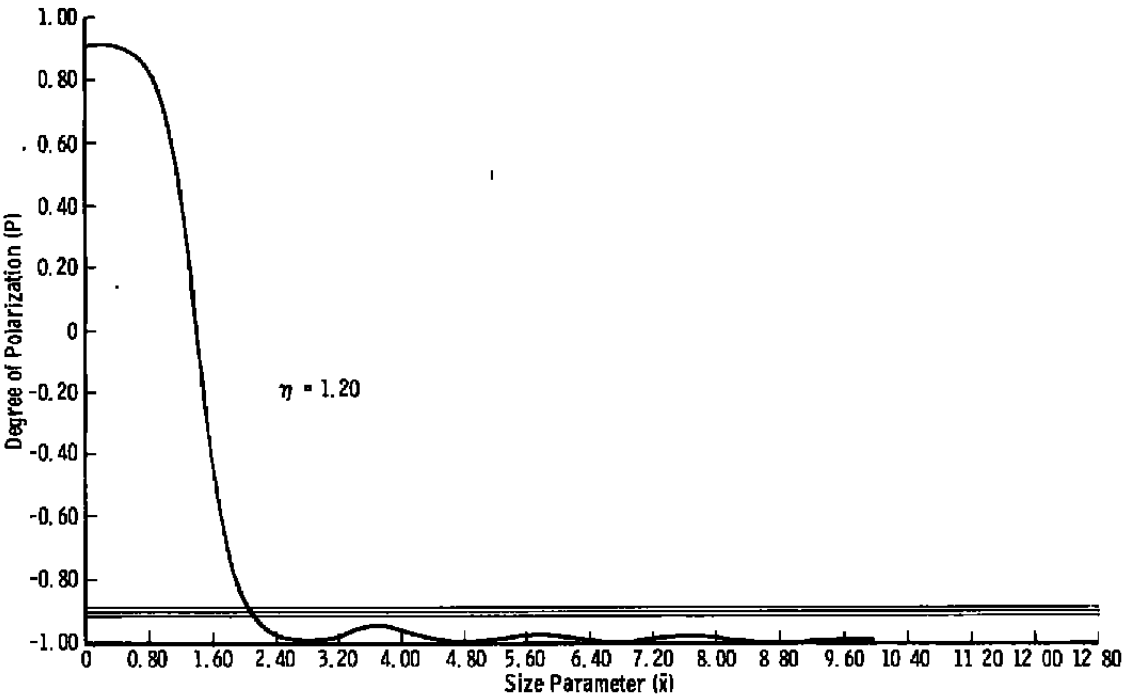

Figure 9. Variation of degree of polarization (P) with size parameter ($\bar{x}$) for particule refractive index of 1.2.

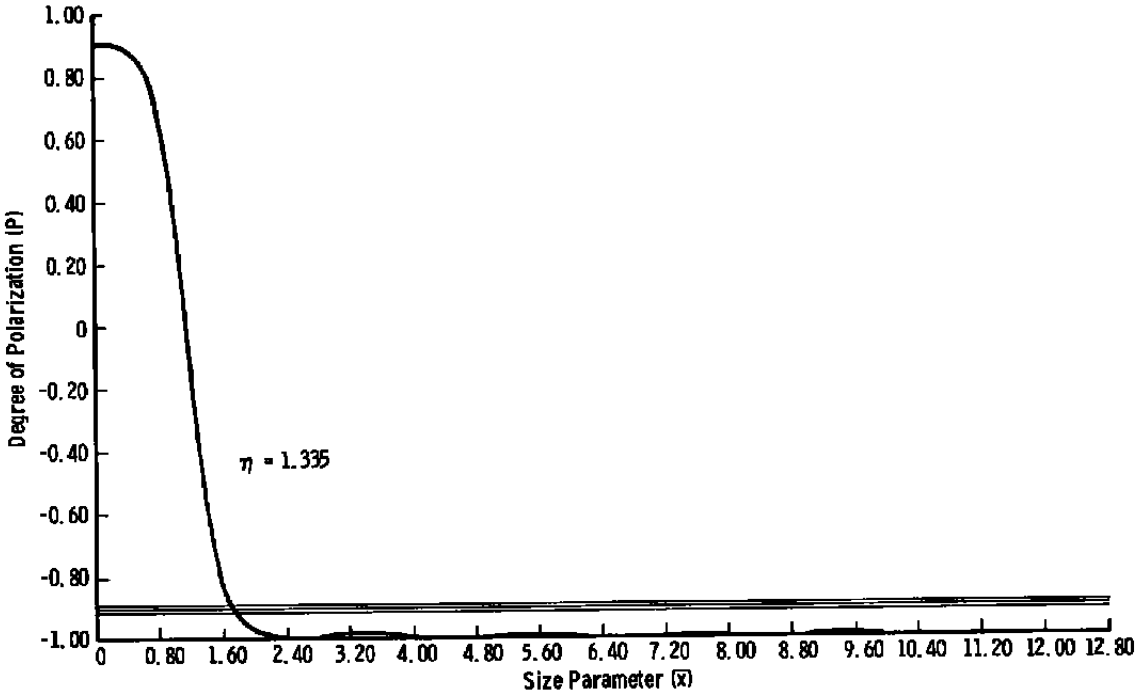

Figure 10. Variation of degree of polarization (P) with size parameter ($\bar{x}$) for particle refractive index of 1.335.

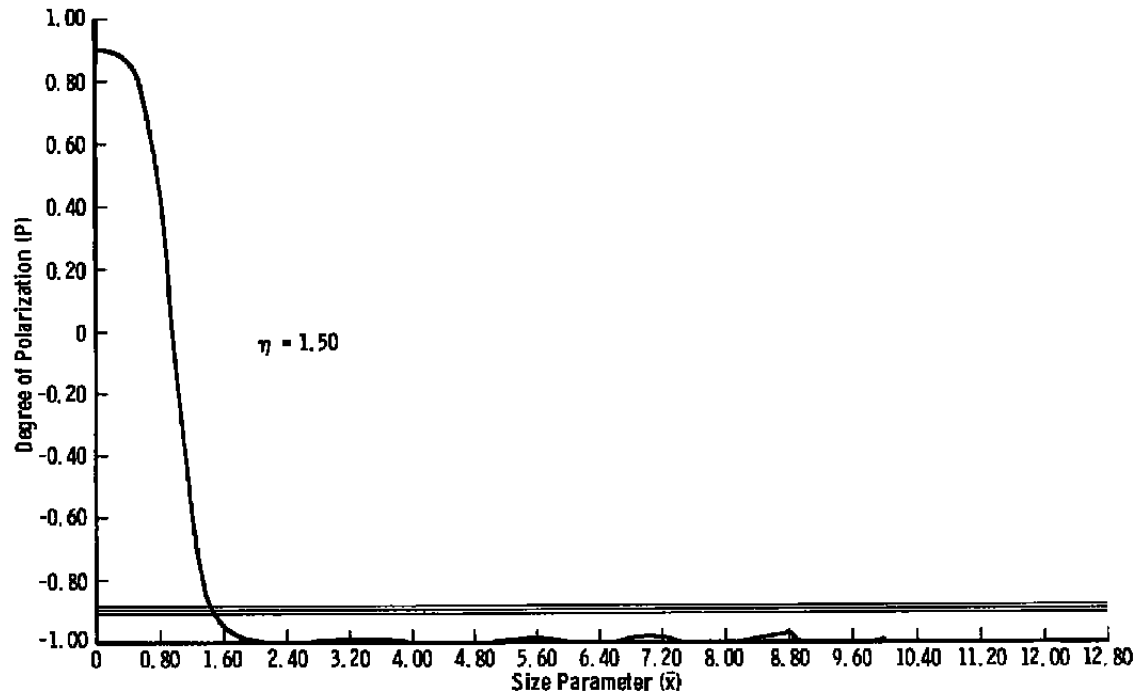

Figure 11. Variation of degree of polarization (P) with size parameter ($\bar{x}$) for particle refractive index of 1.5.

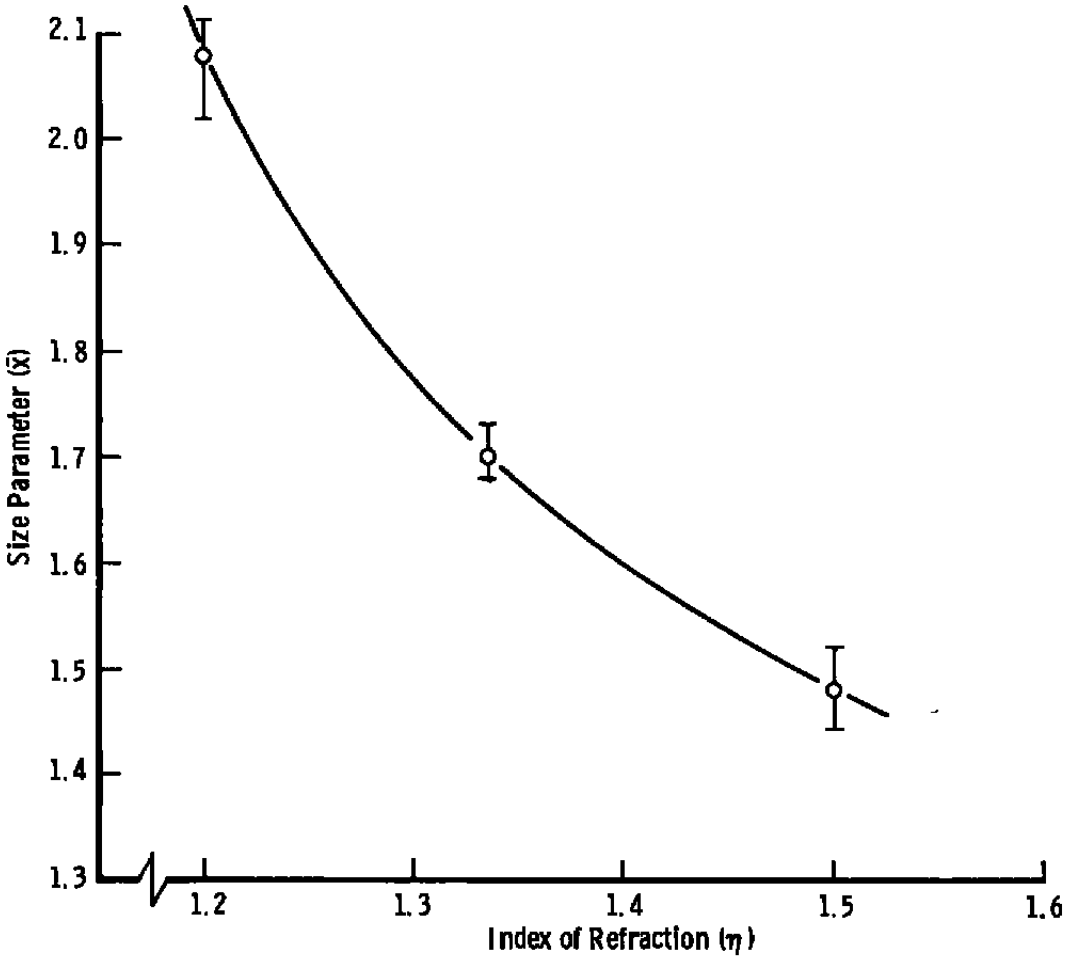

Figure 12. Variation of mean size parameter ($\bar{x}$) with index of refraction (η).

Using this procedure for all the radially dependent data points acquired for the 17-msec firing time enabled the average diameter $\overline{D}$ to be determined, and the results are shown in Fig. 13. From these results it is seen that the measured size parameter ($\bar{x}$) is on the order of 1.75 (which corresponds to a particle diameter of approximately 0.4 μm) and that this result is comparatively constant along the radial direction.

Finally, assuming time-independence of the particle diameter values shown in Fig. 13, the number density (n) of the particles was found from the measured $n\sigma$ products. Figure 14 shows these results for each of the spatially resolved radial positions as a function of engine combustion time.

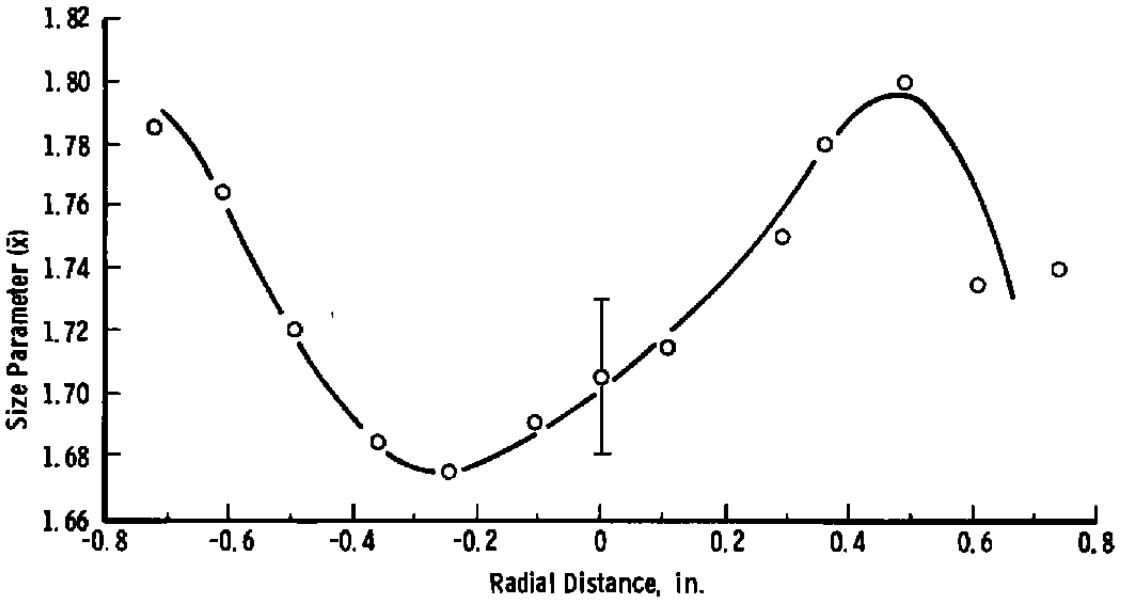

Figure 13. Radial variation of size parameter ($\bar{x}$).

Regarding the uncertainty in the results shown in Fig. 14, one recalls that the imprecision values estimated for the size parameter and particle diameter are less than ±10 percent. Since $\sigma \approx D^3$, the corresponding imprecision values for the number density are on the order of ±30 percent, which characterizes the relative imprecision of the variations of n with respect to pulse time and vertical distance. Further, an estimate of ±100 percent as the order of magnitude of the absolute uncertainty in n is provided by recollection of the uncertainty (±30 percent) in $\bar{x}$ resulting from our ignorance of the exact value of the index of refraction (η).

To obtain an order-of-magnitude estimate of the particulate flux (J_p), one must compute the flow speed at the exit plane of the nozzle. For this purpose it is assumed that at the exit plane of the 100:1 area ratio nozzle the specific heat ratio (γ), the gas species gram molecular weight (M), and the gas temperature (T) are (Ref. 2)

$$\gamma = 1.2,$$

$$M = 30 \text{ gm/mole},$$

and

$$T = 870\text{K}$$

From these estimates one finds the free-stream flow speed to be

$$v_\infty \approx 3 \times 10^5 \text{ cm/sec}.$$

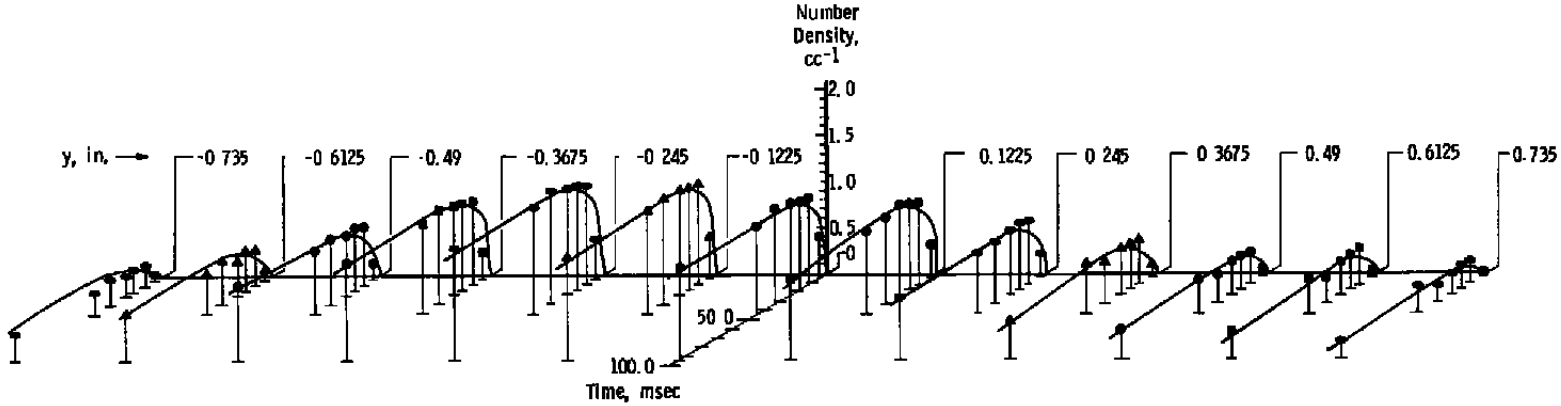

Figure 14. Temporal and radial profiles of particulate number density.

Therefore,

$$J_p = n v_\infty$$

$$\approx 3 \times 10^5 \text{ particles /cm}^2 \text{ /sec,}$$

and the uncertainty in J is on the order of ±100 percent. Since the assumed-liquid particulate bulk density (ϱ_ℓ) is approximately equal to 1 gm/cc, one finds the contaminant mass flux (J_m) to be

$$J_m = \left(\pi \bar{D}^3/6\right) \rho_\ell J_p$$

$$\cong 10^{-8} \text{ gm/ cm}^2\text{/ sec}$$

3.2 COMBUSTION INSTABILITY

It has been shown that the 5-lbf liquid bipropellant engine which was the subject of the study reported in Refs. 1 and 2 achieved steady state with respect to particulate effluent in a characteristic time on the order of 20 to 30 msec. However, there remains the possibility that the existence of combustion instability in the combustion chamber may not be adequately simulated with a short pulse duration of the engine firing. In particular, if the characteristic frequencies of the fundamental acoustical modes of the combustion chamber are sufficiently low and the corresponding characteristic periods are sufficiently large with respect to the engine firing duration, only a portion of the combustion instability will be observed for short pulse firings. Figure 15 sketches this behavior for two cases of combustion instability, and, from Fig. 15, it is seen that inaccurate simulation can result for a low oscillatory eigenmode frequency in the combustion chamber if the engine firing time (τ) is less than the oscillation period. Therefore, it is worthwhile to evaluate the characteristic frequencies and periods for the fundamental oscillation modes of the combustion chamber and to compare these quantities with the engine pulse durations to verify the accuracy of simulation of short engine pulses.

To describe the combustion instability phenomenon the combustion chamber acoustical model will be that of an open Helmholtz resonator. The characteristic oscillation frequencies, f_{ijk}, are given by (Ref. 4)

$$f_{ijk} = (a_o/2) \left[(\alpha_{ij}/R)^2 + (k/L)^2\right]^{1/2} , \quad i, j, k \geq 0 \tag{1}$$

where

a_o = equilibrium (isentropic) speed of sound in the combustion chamber,

R = combustion chamber radius,

and

L = combustion chamber length.

Also, α_{ij} is defined by the zeros of the Bessel function (J_n) derivative as follows:

$$\left[\partial J_n (\bar{\alpha} r R)/\partial r\right]_{r=R} = 0,$$

or

$$J_n'\left(\bar{\alpha}_{ij}\right) = 0 = J_n'\left(\pi \alpha_{ij}\right)$$

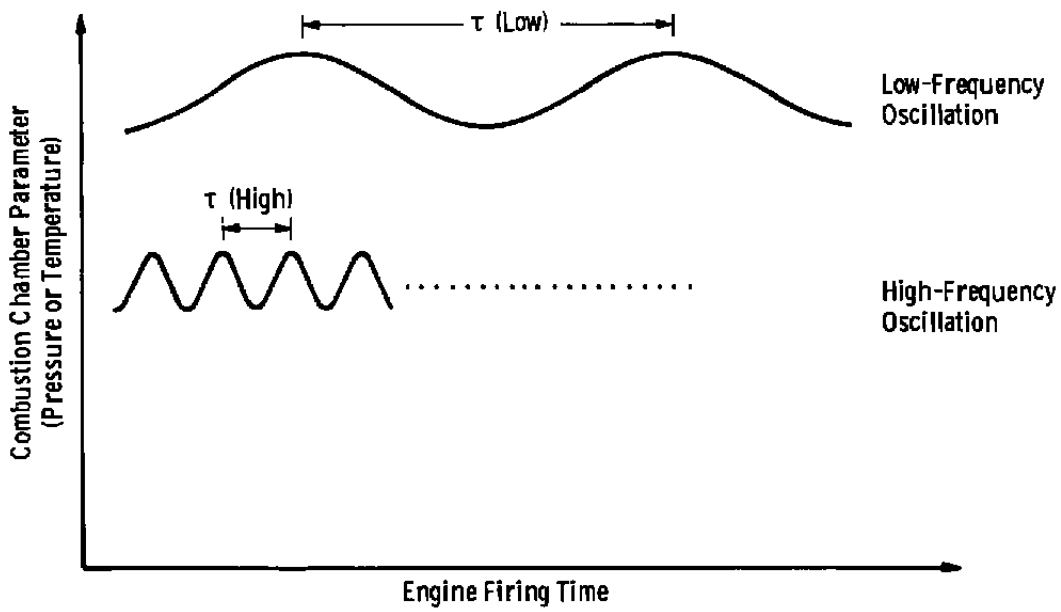

Figure 15. Combustion instability versus engine firing duration.

Equation (1) shows clearly that the lowest characteristic frequencies are the fundamental mode values f_{100}, f_{010}, and f_{001}. If these three frequencies are sufficiently large for a specified engine pulse duration to preclude simulation problems caused by combustion instability, then the even larger harmonic frequencies are definitely inconsequential. Quantitatively, it is demanded that

$$\tau > \tau_{ijk} \equiv 1/f_{ijk} \quad ; \quad i, j, k \geq 0$$

Rewriting Eq. (1) in dimensionless form, one obtains

$$\bar{\tau}_{ijk} \equiv \tau_{ijk} \cdot (a_o/D) = \left[\alpha_{ij}^2 + k^2 (D/2L)^2 \right]^{-1/2} \tag{2}$$

and Fig. 16 shows the variation of $\bar{\tau}_{ijk}$ for the fundamental modes as a function of the ratio L/D. Both the tangential and radial mode quantities $\bar{\tau}_{100}$ and $\bar{\tau}_{010}$, respectively, are independent of L/D, and

$$\bar{\tau}_{001} = 2L/D$$

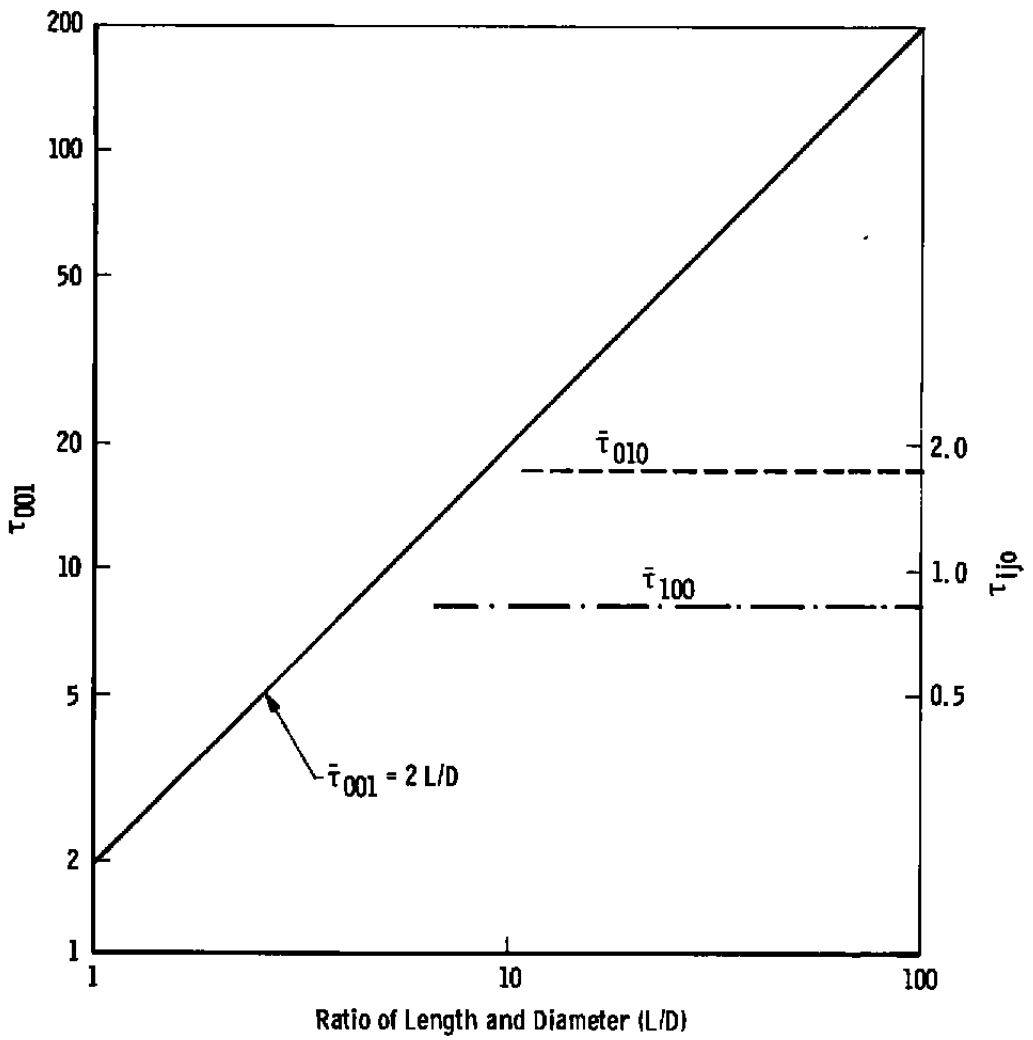

Figure 16. Combustion instability period versus chamber shape factor.

For the engine employed in the studies of Refs. 1 and 2, the combustion chamber diameter and length were 0.50 in. (1.27 cm) and 1.5 in. (3.81 cm), respectively. Estimating the combustion chamber temperature, molecular weight, and specific heat ratio to be 3000°K, 30 gm/mole, and 1.20, respectively, one finds that $a_o \approx 10^5$ cm/sec.

Therefore, one finds that

$$\tau_{100} \approx 1.04 \times 10^{-5} \text{ sec},$$

$$\tau_{010} \approx 2.17 \times 10^{-5} \text{ sec},$$

and

$$\tau_{001} \approx 7.6 \times 10^{-5} \text{ sec} \approx 0\,(10^{-4} \text{ sec}).$$

Since the minimum engine pulse time, τ_{min}, is $0(10^{-3}$ sec),
then

$$\tau_{min} >> \tau_{001} > \tau_{010} > \tau_{100}.$$

Thus, no simulation problems associated with combustion instability are anticipated.

4.0 CONCLUSIONS

The results of this work have shown that: a) the mass density and number density of the particulate effluent of a 5-lbf liquid bipropellant engine attain steady-state characteristics in a time of 20 to 30 msec after initiation of the opening of the propellant valve; b) The particle average size was approximately 0.4 μm and exhibited radial variation at the axial location of 1.1 in. (2.8 cm) relative to the nozzle exit plane; c) Both the radial and temporal variations of the particulate number density (n) were determined, n was found to be on the order of 1 particle/cc, and a slight cylindrical asymmetry was observed; d) The particle mass density was estimated to be on the order of 3×10^{-14} gm/cc, and the order-of-magnitude estimates for mass flux density (J_m) and number flux density (J_p) were found to be 10^{-8} gm/cm^2/sec and 10^5 particles/cm^2/sec, respectively; e) The possibility that combustion instability might affect the accuracy of simulation was considered, and the results indicated that tests using 10-msec engine burn durations could be employed with confidence if the combustion chamber ratio L/D was not more than 30.

In conclusion, it is suggested that the accuracy of simulation of pulsed engine testing with regard to particle kinetics and engine performance has been demonstrated.

REFERENCES

1. Alt, R. E. "Bipropellant Engine Plume Contamination Program, Vol. 1: Chamber Measurements - Phase I." AEDC-TR-79-28 (AD-A077435), December 1979.

2. Powell, H. M., Price, L. L., and Alt, R. E. "Bipropellant Engine Plume Contamination Program, Vol. II: Chamber Measurements - Phase II." AEDC-TR-79-28 (AD-A078412), November 1979.

3. Curry, B. P., Weaver, D. P., and Lewis, J. W. L. "Development of Mie Scattering Techniques for In-Situ Particle Diagnostics at AEDC." AEDC-TR-80-3 (AD-A092716), November 1980.

4. Jackson, J. D. *Classical Electrodynamics.* John Wiley and Sons, New York, 1975, pp. 353-356.

NOMENCLATURE

a_o	Isentropic sound speed in combustion chamber
D	Combustion chamber diameter
$\overline{D}$	Mean diameter of particle
f_{ijk}	Helmholtz resonator characteristic frequencies
J_m	Particulate mass flux
J_n	Bessel function of first kind and order n
J_p	Particulate number flux
k	Acoustic mode wavenumber
L	Combustion chamber length
M	Gram molecular weight of gas species
n	Particulate number density
P	Polarization parameter
R	Radius of combustion chamber

r	Radial coordinate (cylindrical representation)
T	Gas temperature
t	Time
v	Free-stream flow speed
x	Axial position of flow field
$\bar{x}$	Mean diameter of particle
y	Plume radial coordinate perpendicular to axial centerline of flow
α_{ij}	Zeros of Bessel function derivatives
γ	Isentropic ratio of specific heat capacities
η	Refractive index of particle
λ	Wavelength of laser
ϱ_ℓ	Bulk density of liquid
ϱ_p	Particulate mass density
$\sigma(\bar{x})$	Mie scattering cross section
τ	Engine pulse duration
τ_{ijk}	Characteristic period = $1/f_{ijk}$
$\bar{\tau}_{ijk}$	Dimensionless characteristic period = $(a_o/D)\tau_{ijk}$